ACS Biomaterials SCIENCE & ENGINEERING

Article

pubs.acs.org/journal/abseba

3D Printing of Shear-Thinning Hyaluronic Acid Hydrogels with Secondary Cross-Linking

Liliang Ouyang,[†,‡,§] Christopher B. Highley,[†,‡] Christopher B. Rodell,[‡] Wei Sun,[§,⊥] and Jason A. Burdick*[,‡]

[‡]Department of Bioengineering, University of Pennsylvania, Philadelphia, Pennsylvania 19104, United States

[§]Department of Mechanical Engineering, Tsinghua University, Beijing 100084, China

[⊥]Department of Mechanical Engineering and Mechanics, Drexel University, Philadelphia, Pennsylvania 19104, United States

Supporting Information

ABSTRACT: The development of printable biomaterial inks is critical to the application of 3D printing in biomedicine. To print high-resolution structures with fidelity to a computer-aided design, materials used in 3D printing must be capable of being deposited on a surface and maintaining a printed structure. A dual-cross-linking hyaluronic acid system was studied here as a printable hydrogel ink, which encompassed both shear-thinning and self-healing behaviors via guest−host bonding, as well as covalent cross-linking for stabilization using photopolymerization. When either guest−host assembly or covalent cross-linking was used alone, long-term stable structures were not formed, because of network relaxation after printing or dispersion of the ink filaments prior to stabilization, respectively. The dual-cross-linking hydrogel filaments formed structures with greater than 16 layers that were stable over a month with no loss in mechanical properties and the printed filament size ranged from 100 to 500 μm, depending on printing parameters (needle size, speed, and extrusion flux). Printed structures were further functionalized (i.e., RGD peptide) to support cell adhesion. This work highlights the importance of ink formulation and cross-linking on the printing of stable hydrogel structures.

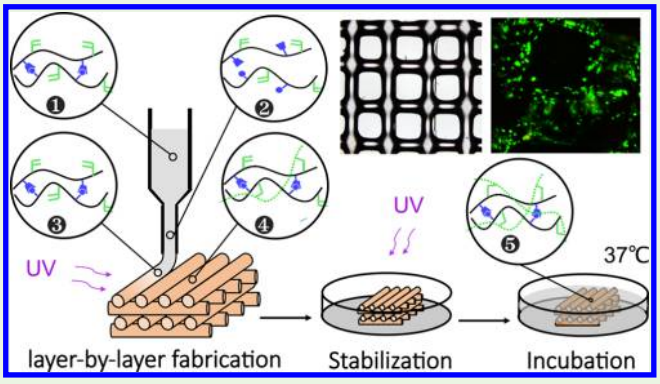

KEYWORDS: *3D printing, hyaluronic acid, hydrogel, guest−host chemistry, photo-cross-linking*

1. INTRODUCTION

The ability to develop three-dimensional (3D) scaffolds is critical for tissue engineering and regenerative medicine applications, as well as for better understanding 3D cell culture environments in vitro. 3D printing (3DP) is evolving as a technique for the fabrication of customized scaffolds with precise control over scaffold structure and properties.[1] Within 3DP, bioinks are printed biomaterials with tunable properties and may contain cells, growth factors, and drugs toward use in various biomedical applications. Despite advances in the field, there still exist challenges in applying 3DP technologies in biomedicine, where the development of materials suitable for use as bioinks is particularly challenging.

Biomaterials that are applied in 3DP must be suited to both the manufacturing process and to the intended biological application. Many biomaterials have been used as bioinks in 3DP processes, including alginate,[2] gelatin,[3] fibrin,[4] collagen,[5] chitosan,[6] and agarose.[7] Each of these biomaterials has specific advantages and disadvantages toward 3DP and combinations of various bioinks can be leveraged to promote their specific advantages and to limit their disadvantages. For example, alginate and gelatin, two of the most commonly used materials in 3DP, have advantages of being well-suited to extrusion and being biocompatible, but they are faced with low cell adhesion and weak mechanical properties, respectively.[8] As components of the native extracellular matrix (ECM), collagen and fibrin could be great bioink candidates, but they both perform poorly in terms of printability and mechanical properties. Thus, the combination of such bioinks can give rise to promising material candidates in 3DP. Given such limitations among existing bioinks, researchers have strived to develop new materials for 3DP.

Hyaluronic acid (HA), or hyaluronan, is a natural glycosaminoglycan that is ubiquitous in almost all connective tissues. As an ECM biomaterial, HA is naturally biocompatible and important in regulating many cellular behaviors and tissue functions, including cell migration, proliferation, differentiation and angiogenesis.[9] Moreover, HA has been used clinically for decades. For these reasons, bioinks based on HA are of interest

Special Issue: 3D Bioprinting

Received: March 20, 2016
Accepted: May 20, 2016

DOI: 10.1021/acsbiomaterials.6b00158
ACS Biomater. Sci. Eng. XXXX, XXX, XXX−XXX

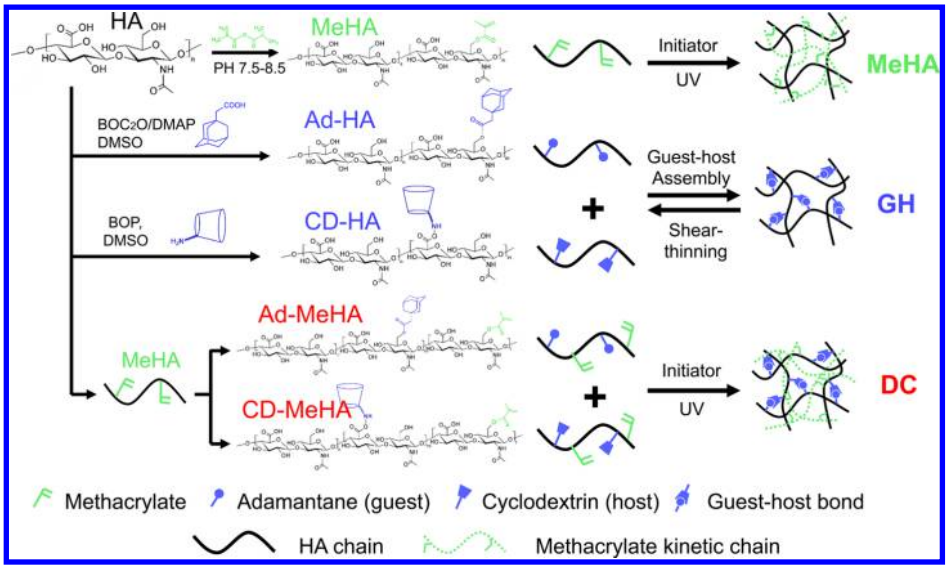

Figure 1. Macromer structures investigated for 3D printing. Modified hyaluronic acid (HA): methacrylated HA (MeHA) for photopolymerization, Ad-HA/CD-HA for guest−host (GH) assembly, and Ad-MeHA/CD-MeHA for dual-cross-linking (DC).

in 3DP. HA has already been included in bioinks through blending with printable hydrogels, including methacrylated gelatin (GelMA),[10] photocurable dextran,[11] and via conjugation with thermoresponsive poly(*N*-isopropylacrylamide).[12] However, unmodified HA is not suitable for 3DP alone, since it exists as a mostly viscous solution that is not stable upon printing. Fortunately, the physical properties of HA can be easily tuned through chemical modifications.[9b,13] Modified HA has been investigated in 3DP including with photo-cross-linkable, methacrylated HA (MeHA), but only as a component of multimaterial ink formulations.[14] Skardal et al. demonstrated numerous HA-based bioink formulations, including the printing of vessel-like constructs in a support-dependent process using MeHA with gelatin,[14c] in printing cross-linked hydrogels composed of poly(ethylene glycol) and thiolated HA,[15] and in printing AuNP-cross-linked HA-gelatin hydrogels.[16]

When applying a new biomaterial ink as in extrusion-based printing, there are numerous considerations that need to be addressed. The primary considerations are printability and stability, which normally encompasses the material's ability to (i) be extruded from a printhead and deposited on a surface, (ii) to undergo rapid gelation upon deposition, and (iii) to exhibit mechanical properties that support the printed structure. It remains a significant challenge to meet these criteria in printable materials and particularly with hydrogels. To address these criteria, we applied a shear-thinning and rapidly self-healing guest−host hydrogel based on HA[17] to 3DP. Briefly, adamantane (Ad, guest) and β-cyclodextrin (CD, host) moieties were separately coupled to HA, to create two hydrogel-precursors that formed a supramolecular assembly upon mixing. To enhance the structural integrity of the supramolecularly cross-linked hydrogel, we also introduced photo-cross-linkable methacrylate groups onto the macromers. We then investigated how each type of cross-linking (guest−host, photo-cross-linking, and their combination) affected the printability of multilayer scaffolds. In summary, we introduce here a novel HA-based hydrogel ink for traditional extrusion-based 3DP that allows for fabricating complex HA scaffolds.

2. MATERIALS AND METHODS

2.1. Materials Synthesis. Modified hyaluronic acid (HA) macromers were synthesized based on sodium HA (90 kDa, Lifecore) as previously described.[17a] In brief, Ad-HA was prepared through anhydrous coupling of 1-adamantane acetic acid to the tetrabutylammonium salt of HA (HA-TBA) via di*tert*-butyldicarbonate (Boc_2O)/4-dimethylaminopyridine (DMAP) esterification in DMSO. CD-HA was prepared by coupling 6-(6-aminohexyl)amino-6-deoxy-β-cyclodextrin (β-CD-HDA) to HA-TBA via an amidation reaction using (benzotriazol-1-yloxy)tris(dimethylamino)phosphonium hexafluorophosphate (BOP) in anhydrous DMSO. MeHA was prepared through the reaction of HA with methacrylic anhydride as reported.[18] Adamantane-modified MeHA (Ad-MeHA) and cyclodextrin-modified MeHA (CD-MeHA) were generated by sequential combinations of these processes (Figure 1). The modification percentage of adamantane, β-cyclodextrin and methacrylates for the modified macromers were 21, 25, and 22%, respectively, which were determined by ^{1}H NMR (Bruker 360 MHz) (Figure S1A).

To fluorescently label printed materials, we conjugated Ad-MeHA to thiolated 5(6)-carboxyfluorescein (GCKKG-fluorescein) via a Michael addition reaction as previously described.[19] In short, Ad-MeHA and the thiolated fluorophore were dissolved in a 0.2 M triethanolamine buffer (TEOA) at pH 8.0 and reacted overnight at 37 °C. Fluorescently labeled Ad-MeHA was subsequently purified by dialysis and lyophilized.

2.2. Hydrogel Preparation. All HA macromers were dissolved in PBS. For methacrylated HA macromer (MeHA, Ad-MeHA and CD-MeHA) solutions, the photoinitiator Irgacure 2959 ((4-(2-hydroxyethoxy)phenyl-(2-propyl)ketone, I2959) was included at a concentration of 0.05 wt % for photopolymerization. For guest−host based mixtures (Ad-HA/CD-HA and Ad-MeHA/CD-MeHA), individual macromer solutions were formulated and mixed completely such that the Ad and CD moieties were present at a one-to-one ratio. Three basic hydrogel groups (Figure 1) were used, namely MeHA (Photo cross-linking, MeHA), Ad-HA/CD-HA (Guest−Host, GH), and Ad-MeHA/CD-MeHA (dual-cross-linking, DC), whose macromer concentrations varied from 5 to 20 wt %. For those materials being used in cell culture, the raw materials were sterilized with a germicidal light for 30 min.

2.3. Rheological Characterization. Rheological measurements were performed at 25 °C on an AR2000 rheometer (TA Instruments) using a cone−plate geometry (20 mm diameter, 59 min 42 s cone angle, and 27 μm gap). To evaluate rheological properties, material responses to shear were examined in continuous flow experiments with a linearly ramped shear rate from 1 to 100 s^{-1}. Responses to increasing

DOI: 10.1021/acsbiomaterials.6b00158
ACS Biomater. Sci. Eng. XXXX, XXX, XXX−XXX

strain were measured with oscillatory strain sweeps from 0.01 to 500% strain at 10 Hz. The frequency dependence of material properties to the application of strain were measured with oscillatory frequency sweeps from 0.01 to 100 Hz at 0.2% strain. The material responses to the application and removal of shear were examined in shear recovery experiments, where oscillatory (10 Hz) time sweeps were conducted with alternating high/low strains of 250/0.5% every 2 min. To measure the response of rheological properties to photopolymerization, in situ polymerization was performed with 15 mW/cm^2 ultraviolet (UV) light using an Exfo Omnicure S1000 lamp with a 320−390 nm filter for 5 min via a UV-curing stage during oscillatory time sweeps at frequency 1 Hz and strain 0.5%.

2.4. 3D Printing Process. A hydrogel-based extrusion 3DP system was used as previously described.[19] Briefly, we designed and fabricated a stepper motor-driven piston-based nozzle suitable for extrusion on a commercial 3D FDM printer (Revolution XL, Quintessential Universal Building Device). Standard software was used to generate G-code (Slic3r) based on STL files representing 3D CAD models (AutoCAD) and to control printing hardware (Repetier), communicating the commands to direct the layer-by-layer printing movements. Parameters such as extrusion flux, moving speed, and printed structure were easily changed in G-code. Unless otherwise stated, the printing process was performed at room temperature with an extrusion flux of 0.33 mL/h, moving speed of 1.5 mm/s, filament gaps of 1 mm, and needle gauge of 25G. After the ink was loaded into the syringe, the transparent parts of the syringe and needle were wrapped with aluminum foil to prevent premature photopolymerization. Once the printing started, UV light was directed at the printing area during the course of the print with an intensity of 15 mW/cm^2, unless otherwise stated.

2.5. Stabilization Process. An additional UV treatment process was applied to the printed structures for stabilization postprinting. All printed structures for UV cross-linking contained 0.05 wt % I2959 and were irradiated during printing as described above. We applied four different postprint protocols to optimize construct stabilization by irradiating printed structures containing 0.05 wt % I2959 in different environments. These stabilization protocols (SP-1, SP-2, SP-3, and SP-4) each involved a total of 5 min of UV irradiation postprinting. In SP-1, printed structures were irradiated entirely under the ambient air atmosphere for 5 min. In SP-2, structures were irradiated under air for 2.5 min and then immersed into PBS and irradiated for 2.5 min. In SP-3, the procedure was the same as SP-2, except that the PBS included 0.05 wt % I2959. In SP-4, printed structures were immersed in PBS containing 0.05 wt % I2959 for the entire 5 min irradiation time. After postprinting stabilization, all structures were subsequently immersed into PBS for incubation at 37 °C. A fluorescent microscope (Olympus BX51) was used to capture the fluorescence and bright-field images of structures during one-month incubation.

2.6. Filament Characterization. To better understand the cross-section of the actual filament, it was presumed to be elliptical in shape and we used the ratio (n) of the short-axis (b) to long-axis (a) to assess the inks' ability to maintain the printed shape. Therefore, the area of the cross-section, A, could be expressed as

$$A = \frac{1}{4}\pi ab = \frac{1}{4}\pi n a^2 \quad (1)$$

On the other hand, according to the extrusion parameters we can obtain the following equation based on volume conservation

$$V = Avt = Qt \quad (2)$$

where V is the volume of the filament, v is the moving speed of nozzle, t is the printing time and Q is the extrusion flux. Combining eqs 1 and 2, we can evaluate the n value as the following

$$n = \frac{4Q}{\pi a^2 v} \quad (3)$$

where a is measured through fluorescent images using the Measurement tool in the DP2-BSW software of the microscope (Olympus BX51). Parameters were varied to investigate differences in the filament size with extrusion flux from 0.04 to 0.4 mL/h, needle gauge from 22G-30G, and moving speed from 1 to 5 mm/s. A value of $n = 1$ is indicative of a circular cross-section. All of the size measurements were taken immediately after printing with at least four filaments for each sample.

2.7. Mechanical Testing. A cylindrical structure with a diameter of 6 mm and a length of 1.8 mm was designed and printed for compression testing. The tests were performed using a dynamic mechanical analysis system (Q800, TA Instruments) with strain linearly ramped from 0 to −25% at the rate of −10%/min. Compressive moduli were determined by linear fitting (R^2 of 0.94 to 0.99) of the stress−strain curve in the strain region between −10 and −20%. Samples were prepared in triplicate for each test.

2.8. Cell Seeding and Culture on Scaffolds. After printing and cross-linking, as described above, Ad-MeHA/CD-MeHA scaffolds for use in cell seeding were functionalized with the cell adhesive peptide, RGD. Printed scaffolds were incubated overnight at 37 °C in 0.2 M TEOA buffer (pH 8.0) with 2 mM of the oligopeptide GCGY*RGD*SPG, which contains the RGD adhesion sequence and a cysteine residue to allow a Michael addition reaction with unreacted methacrylates and thiols.

NIH 3T3 fibroblasts were expanded in growth medium (α-MEM, 10% FBS, 1% L-glutamine and 1% penicillin-streptomycin) and applied directly onto the RGD-functionalized scaffolds by immersing scaffolds in suspensions of 2 million cells/mL at passage 10 or less. Cell-seeded scaffolds were cultured in growth medium for 5 days prior to imaging with calcein-AM/ethidium homodimer (Live/Dead) staining.

3. RESULTS AND DISCUSSION

3.1. Material Development and 3DP Process. Several HA macromers were synthesized, namely, MeHA, Ad-HA, CD-HA, Ad-MeHA, and CD-MeHA at modification levels of ∼20−25% of the HA repeat units (Figure 1). The methacrylate group allows for cross-linking via a photoinitiated free-radical polymerization, whereas the Ad and CD modifications permit supramolecular assembly through the formation of guest−host pairs. Toward application in 3DP, a process was developed that harnessed the shear-thinning and self-assembling process of the guest−host hydrogels and the stabilization afforded with photopolymerization of the methacrylate groups. The general process is outlined in Figure 2 A. This involves a shear-thinning and self-healing guest−host hydrogel (Ad-MeHA and CD-MeHA) loaded into a syringe for extrusion, the disassembly of the gel at the interface between the gel and syringe with extrusion and shear, and the self-healing of the gel upon injection onto a substrate. With light exposure and in the presence of an initiator, covalent cross-links were subsequently introduced to stabilize the printed structures (dual-cross-linking, DC). Control hydrogels that incorporated only the MeHA macromer (no guest−host assembly) or only the Ad-HA and CD-HA (no covalent cross-linking) were also investigated. Methacrylate modification was targeted to be approximately 20%, as this was known to result in rapid covalent cross-linking. Guest−host modifications were targeted to be approximately 25%, as higher modifications led to networks that were more difficult to extrude through the needle.

Previous work in our lab has explored the use of such materials in 3DP,[19] but with a unique procedure, where supramolecular properties allowed the printing of one material directly into another. This allowed the printing of material anywhere in 3D space, including as pockets of material, filaments, or with multiple inks within the same hydrogel. Additionally, we used the photostabilization process to permit formation of channels within hydrogels or free-standing 3D-

DOI: 10.1021/acsbiomaterials.6b00158
ACS Biomater. Sci. Eng. XXXX, XXX, XXX−XXX

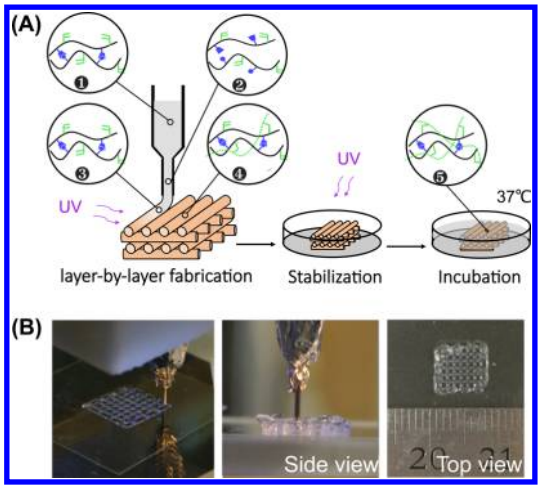

Figure 2. 3D printing process. (A) Schematic of 3D printing, stabilization, and incubation processes for DC hydrogels. The steps include: (1) supramolecular hydrogel assembly with guest−host bonds within the syringe chamber; (2) guest−host bond disruption when extruded through the narrow needle, due to shear; (3) rapid self-healing of the supramolecular hydrogel and guest−host bonds when shear is removed and the material is deposited; (4) UV treatment to photo-cross-link methacrylates within the printed hydrogels; and (5) stabilization to enforce the polymerized network. (B) Representative images of the printing process and a printed multilayer structure.

structures. Here, we investigated these materials in the formation of self-supporting filamentous structures, with a focus on the dual-cross-linking system to obtain 3D stable structures (Figure 2B). This combination of cross-link types represents an important consideration in the design of biomaterials for 3DP in layer-by-layer approaches.

3.2. Rheological Evaluation. The rheological properties of supramolecular hydrogels are central to their use as injectable biomaterials[17a,20] and when used as either support materials or bioinks in 3DP applications.[19] The requirements for extrusion of these materials as filaments in standard layer-by-layer 3DP can be different, as the filament needs to be extruded from a syringe, resist deformation after printing, and maintain structural integrity over the lifetime of the printed construct. Consequently, a variety of rheological properties were determined for the various ink candidates investigated.

Time sweeps of modified HA macromer solutions showed that at a frequency of 10 Hz and strain of 0.5%, the modulus of MeHA, Ad-HA, and CD-HA solutions were low, no more than 50 Pa, and the storage modulus (G') was generally lower than the loss modulus (G''), reflecting properties of viscous solutions. Significantly higher G' and G'' values (~1000 Pa) were observed when Ad-HA and CD-HA were combined to form a hydrogel, with G' higher than G'' (Figure 3A), indicative of gelation by supramolecular cross-linking. The continuous flow experiments show that the viscosity of GH materials decreased with increasing shear rate under different concentrations, demonstrating shear-thinning, with viscosity under high shear similar to that of an uncross-linked MeHA solution (Figure 3B). The viscosity of MeHA was lower than GH materials and remained constant as a function of shear rate, reflecting properties of a Newtonian fluid (Figure 3B). Moreover, for GH materials, G'' surpassed G' beyond the linear viscoelastic region (LVR) at high strains in oscillatory strain sweep tests (Figure S2A), indicative of shear-yielding, which is essential for hydrogel extrusion. It was observed that the strain at which G'' exceeded G' increased with increasing macromer concentration. The oscillatory frequency sweep tests also showed that the GH materials underwent a conversion

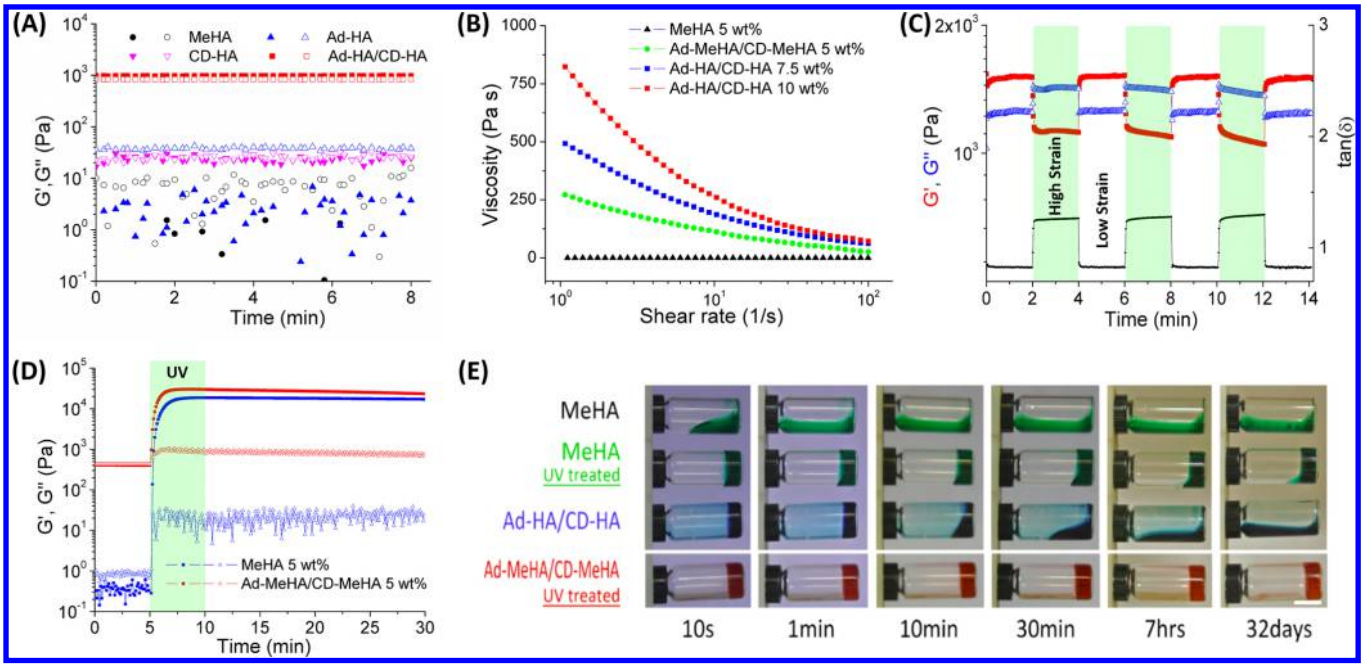

Figure 3. Rheological properties and relaxation behavior of hydrogels. (A) Oscillatory time sweeps of different modified HA macromers (frequency 10 Hz and strain 0.5%), G' (closed symbols) and G'' (open symbols). (B) Continuous flow tests of MeHA and GH materials at shear rates equivalent to those experienced during printing, showing shear-thinning behavior with viscosities of GH assemblies approaching that of the MeHA solution at high shear rates. (C) Cyclic strains of 0.5% (low, unshaded area) and 250% (high, shaded area) at 10 Hz for the 5 wt % DC hydrogel prior to light exposure. (D) Time sweep of photo-cross-linking with UV exposure (15 mW/cm^2 for 5 min as indicated by shaded area), G' (closed symbols) and G'' (open symbols). (E) Images of various hydrogels (all at 5 wt %) in vials on their side for up to one month. Scale bar is 10 mm.

DOI: 10.1021/acsbiomaterials.6b00158
ACS Biomater. Sci. Eng. XXXX, XXX, XXX−XXX

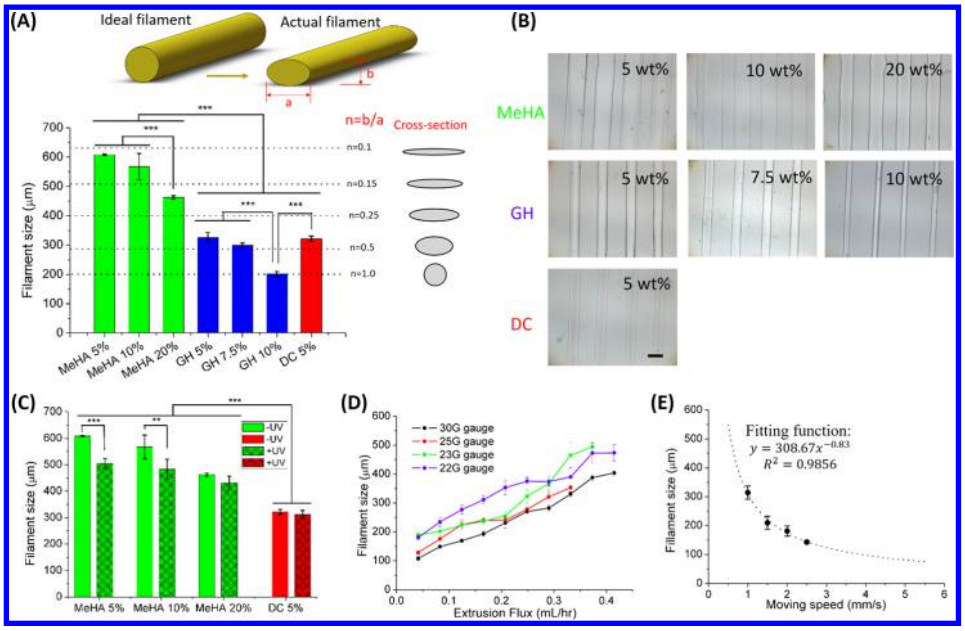

Figure 4. Characterization of printed filaments. (A) Quantification and (B) visualization of filament sizes for MeHA, GH, and DC hydrogels under the same printing parameter configuration (extrusion flux of 0.22 mL/h, 25G needle, moving speed of 2 mm/s) at varied concentrations. (C) Filament sizes with UV exposure (15 mW/cm^2) during printing (~50 s) for MeHA and DC hydrogels. (D) Filament sizes (5 wt % GH hydrogel) with variations in extrusion flux and needle gauge with a fixed moving speed (1.5 mm/s). (E) Filament sizes (5 wt % GH hydrogel) with variations in moving speed under fixed extrusion flux (0.14 mL/h) and needle gauge (25G). All results are presented as the mean ± standard deviation (SD), unless otherwise stated. Statistical significance was defined as $^*p < 0.05$, $^{**}p < 0.01$, $^{***}p < 0.001$ using one-way analysis of variance (ANOVA) in conjugation with a Bonferroni posthoc test. Scale bar is 500 μm.

from fluid-like to solid-like behavior with increasing frequency in a concentration-dependent manner (Figure S2B), indicating that fluid-like settling of GH hydrogels may occur over long time scales and is slowed by increased polymer concentration.

When investigated under alternating low/high strains, the DC hydrogels went from solid-like to fluid-like behavior in response to strain prior to photo-cross-linking. Furthermore, the responses to high strain and mechanical recoveries at low strain were rapid and repeatable (Figure 3C). In combination with the shear-thinning properties, this rapid transition from solid-like to liquid-like behavior as strain is applied makes the hydrogel material well-suited for extrusion-based bioprinting. The rapid recovery of mechanical properties after removal of shear, as during deposition of a filament, allows for stabilization of the printed filaments immediately after extrusion. When hydrogels containing methacrylates were exposed to light, rapid polymerization was observed with a multiple orders of magnitude increase in storage modulus (Figure 3D). The relaxation behavior of the hydrogels was dependent on the type of cross-link (Figure 3E). As a control, low viscosity, unpolymerized MeHA flowed immediately, whereas GH hydrogels with only guest−host bonds relaxed gradually over several hours. Importantly, GH hydrogels composed of HA modified approximately 20−25% with adamantane or cyclodextrin were observed to maintain their shape on the same order of time—minutes—over which photopolymerization occurs. After photopolymerization, both the MeHA and DC hydrogels kept their shape for up to one month. This rapid covalent cross-linking in response to UV irradiation, allows printed filaments to be stabilized against forces that otherwise could cause rearrangement or dispersion of the hydrogel over time. Other methods of introducing covalent cross-links (e.g., thiol−ene reactions) or incorporation of enzymatically degradable cross-links will allow optimization to specific applications.

3.3. Filament Characterization. The strengths of a combined supramolecular and photoinduced cross-linking system to enable the printing of stable hydrogel filaments are further confirmed by characterization of filament shapes after printing. In order for a 3D structure to be correctly translated from a computer model to a material construct via 3DP, the filament shape should reflect the original design. The filament should ideally have a circular cross-section and not flatten after printing so that it forms the desired structure, including the spacing between filaments.

The three ink types (MeHA, GH, DC) were evaluated for application in depositing filaments using the process outlined in Figure 2 and at varied concentrations. Generally, continuous filaments of uniform size were printed, which required consistent force for extrusion (Figure S3). The results demonstrated that the filament widths of guest−host based inks (GH and DC) were significantly smaller than that of the MeHA ink when viewed from above (Figure 4A, B). In other words, the n value of the GH-based ink was closer to 1 than that of the MeHA ink. This indicates that the GH assembly is able to limit the material collapse upon printing, when compared to the MeHA solution alone, which disperses upon extrusion. Specifically, for a macromer concentration of 5 wt %, the filament sizes of the MeHA, GH and DC inks were 608.4 ± 1.8, 325.7 ± 17.6, and 321.8 ± 9.5 μm, respectively. Furthermore, with higher macromer concentrations, the size of the filament, as viewed from above, decreased. In particular, GH hydrogels at 10 wt % were observed to have an n value closest to 1, which meant that the cross-sectional outline of the filament was nearly circular. When treated with UV during material deposition, the MeHA filaments experienced a significant decrease in size when observed from above, for

DOI: 10.1021/acsbiomaterials.6b00158
ACS Biomater. Sci. Eng. XXXX, XXX, XXX−XXX

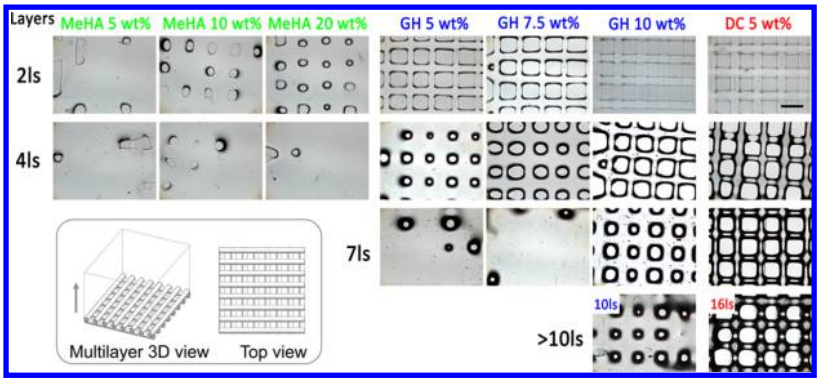

Figure 5. Printing of 3D structures. Phase images of printed grid structures (CAD model shown as inset) with different layers for MeHA, GH and DC hydrogels (MeHA and DC groups were treated with 15 mW/cm^2 UV) at various concentrations. The number of layers (ls) printed is indicated (left) as well as hydrogel concentration (top). Scale bars are 1 mm.

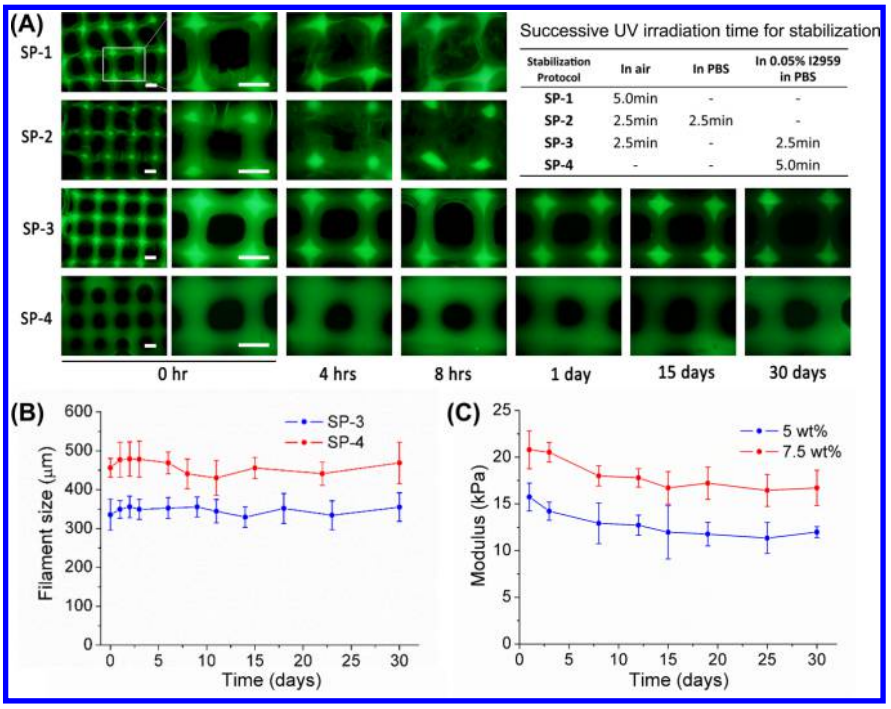

Figure 6. Stabilization procedures of printed DC structures. (A) Fluorescence images of printed structures treated with different stabilization protocols (shown in table) for up to one month. (B) Filament size of printed DC hydrogels with incubation time for SP-3 and SP-4 stabilization protocols. (C) Compressive moduli of printed DC hydrogel structures following SP-3 protocol with incubation time at two concentrations. Scale bars are 500 μm and represent the same magnification in the far left column and then a higher magnification for all other images.

concentrations of 5 and 10 wt % (Figure 4C). However, the filament size of the MeHA ink was still larger than that of the DC ink. Thus, although UV irradiation during printing of methacrylated macromers increased circularity (Figure 4C), the rapid reassembly of the supramolecular bonds after printing was needed to achieve a cross-section that approached ideal circularity.

Using the GH ink, the filament size was investigated with changes in printing parameters. The results showed that the filament size increased with the increase of extrusion flux and that, generally, a smaller needle (increased gauge) resulted in smaller filaments (Figure 4D). Under fixed extrusion flux and needle gauge, the filament size decreased as the needle's speed increased, and the relationship curve was well-fit (R^2 of 0.99) by a power law (Figure 4E). However, when the translational speed was too high, the filament was not continuous (Figure S4). In general, the filament size ranged from 100 to 500 μm through modulation of these parameters. Filament size can therefore be controlled and tuned as needed for a particular printed structure, through extrusion flux, needle size, and, within limits, by the rate of translation of the needle. Although the filament size could be varied within a single printed construct, this capability was not explored here. The ability to print thinner filaments from larger diameter needles by tuning needle speed might, for example, offer the ability to increase print resolution while minimizing shear forces experienced by an ink.

3.4. 3D Printed Structures. The benefits of the dual supramolecular-covalent cross-linking system in stabilizing printed filaments were clearly observed as layers of a 3D structure were deposited upon one another (Figure 5). Different layers of grid structures were printed layer-by-layer using the various inks to evaluate their printability, with MeHA and DC groups receiving UV irradiation during the printing

DOI: 10.1021/acsbiomaterials.6b00158
ACS Biomater. Sci. Eng. XXXX, XXX, XXX−XXX

process. As shown in Figure 5, the MeHA ink, stabilized only by UV-induced cross-linking, did not gel fast enough to avoid flow and coalescence. This ink could not deliver a clear grid structure even with only two printed layers, and all of the filaments had coalesced when four layers had been printed.

Using GH inks, relaxation and coalescence of printed filaments were ultimately observed as layers were deposited, although more layers could be deposited while maintaining a clear grid structure when compared to the MeHA group. Increasing the concentration of the GH ink resulted in better performance when compared to lower concentrations. Specifically, GH-5 wt % and GH-7.5 wt % groups coalesced after only seven layers had been deposited. Although a grid structure was identified in a ten-layer construct fabricated from the GH-10 wt % ink, the filaments were still obviously fused together, with increasingly small void spaces between the filaments in the grid.

When the DC ink was used at a concentration of 5 wt %, a standard multilayered structure (up to 16 layers are shown in Figure 5 and more in Figure S5) was possible. Thus, the combination of the guest−host assembly and the secondary cross-linking was needed to preserve the printed structures in multilayer scaffolds. Structures stabilized by supramolecular interactions formed well-spaced filaments that were stable in the short term, as evidenced by the two layer prints of the GH and DC groups. However, the covalent cross-linking mechanism was necessary to stabilize printed structures against relaxation of the supramolecular network and resulting flow of material that was evident in all of the GH groups. The DC mechanism yielded stable structures that maintained spatial fidelity to the computer model for as many layers as were printed.

3.5. Enhancing Structure Stability. Various stabilization protocols were investigated to further enhance the stabilization of the printed structures. When structures were irradiated with UV light for 5 min under ambient air and subsequently placed into PBS—the first stabilization protocol, SP-1—changes in the structure were observed over time (Figure 6A). It is known that the conditions under which radical-induced polymerizations are performed are critical to the formation of covalent bonds throughout the hydrogel. Specifically, oxygen competitively reacts with the radicals generated by the photoinitiator (I2959) that are needed to initiate and propagate the polymerization. Thus, light exposure in ambient air may not have induced complete cross-linking throughout the structures, which limited stability and led to erosion (Figure 6A). The same results were observed in structures treated first with UV light in the air and then with UV light after immersion in PBS for 2.5 min each (SP-2); however, any remaining initiator may have diffused from the structure prior to the second round of light exposure, limiting any added stabilization. The use of these protocols did not lead to long-term stability of printed structures.

When 0.05 wt % photoinitiator was included in the PBS during the second 2.5 min irradiation (SP-3), the grid structure was observed to have clear edges even up to one-month incubation. The fourth protocol (SP-4), immersion in PBS containing 0.05 wt % I2959 for the whole 5 min irradiation, also supported the structure for one month. However, the filament sizes with this protocol (SP-4) were significantly larger than that of samples in SP-3. This was likely a result of relaxation of the network and/or hydrogel swelling prior to the light exposure. Thus, the SP-3 protocol is best to maintain printed structures. Once covalently cross-linked, printed structures were stable over time, with filament sizes (Figure 6B) and mechanical properties (Figure 6C) changing little over a one-month incubation period. Specifically, the modulus decreased from 15.7 ± 1.5 to 12.0 ± 0.6 kPa and from 20.8 ± 2.0 to 16.7 ± 1.9 kPa from day 1 to day 30 for samples printed with macromer concentrations of 5 and 7.5%, respectively (Figure 6C).

Printing the DC ink using these procedures allowed the rapid fabrication of many structures, including stable tubes and hydrogel sheets (Figure S5). These structures were stable in aqueous medium at 37 °C, with no noticeable change in gross appearance over a month (Figure S6). This indicates the potential for this hydrogel ink to be used as a substrate for the creation and maturation of engineered tissue constructs. Although not investigated here, it should be noted that the potential exists—and has been previously demonstrated in HA hydrogels—for the cross-links used here to have designed degradation profiles, where cross-links are susceptible to hydrolysis[21] or enzymatic degradation,[22] including cross-links formed by guest−host assembly.[17b]

3.6. Cell-Seeded Constructs. In addition to considerations of the printability of the biomaterial components and the stability of the printed structure, rapidly fabricated high-resolution scaffolds are of interest for the culture of cells. Here, printed scaffolds were functionalized with RGD and seeded with 3T3 fibroblasts to assess their potential to support cell culture. The modification of dual-cross-linking scaffolds to support cell attachment was achieved through the methacrylate moieties on the HA-backbone, which offers an accessible handle for further modification of hydrogels after gelation. RGD was necessary for cell adhesion to the scaffolds.

While many functionalities might be introduced, here the conjugation of RGD peptides to the 3D printed scaffolds allowed cell attachment to the surface of the printed constructs. Specifically, scaffolds were imaged after 5 days in culture (Figure 7A, B) by staining cells using calcein-AM (green) and ethidium homodimer (red). 3D printed scaffolds supported cell adhesion, with cells extending projections and spreading across filaments (Figure 7B). In this initial study, the cells were seeded through simply immersing the scaffold in cell suspensions. Ongoing and future work will continue to investigate how material properties might be tuned for use with cells, in the context of 3DP as well as other applications of the supramolecular materials. Fully understanding the non-Newtonian shear forces within the gels and controlling them through material formulation and the modification of current

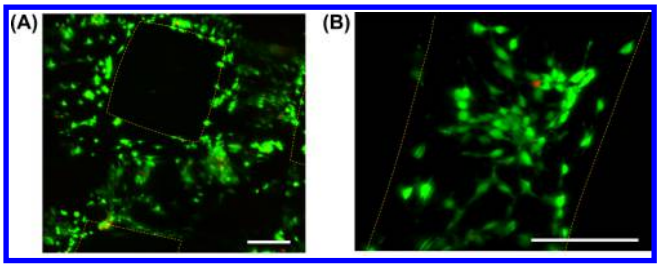

Figure 7. Cells seeded onto RGD-functionalized DC hydrogel scaffolds. (A) Maximum projection from a confocal *z*-stack of fibroblasts adhered to a DC scaffold and stained for viability with live/dead stain. (B) Magnified view of cells spreading on the surface of a filament. Scale bars are 200 μm.

DOI: 10.1021/acsbiomaterials.6b00158
ACS Biomater. Sci. Eng. XXXX, XXX, XXX−XXX

printing technology will expand possibilities for use of these materials as bioinks.

4. CONCLUSION

HA macromers were used as printable hydrogels in extrusion-based 3D printing, and the type of cross-linking led to differences in printed filament outcomes and stability. A dual-cross-linking strategy allowed rapid stabilization of printed filaments by supramolecular bonds immediately upon extrusion, which induced short-term stability until covalent cross-linking resulted in further stabilization. Printed structures were then stable for up to a month of incubation. Control hydrogel inks that consisted of covalent cross-linking or supramolecular interactions alone either lost the printed filament structure or were not stable after a few layers. The dual-cross-linking strategy does not require the use of other support materials, such as alginate or gelatin, allowing the HA-based system to be designed to a specific application, without having to introduce a secondary material. Because the HA backbone structure allows for multiple modifications, an HA derivative engineered for use in cartilage[23] or cardiac[24] tissue engineering might be readily adapted to 3DP using this approach, as might other hydrogels where supramolecular and covalent cross-linking chemistries can be combined.

■ ASSOCIATED CONTENT

Supporting Information

The Supporting Information is available free of charge on the ACS Publications website at DOI: 10.1021/acsbiomaterials.6b00158.

Figures S1−S6 (PDF)

■ AUTHOR INFORMATION

Corresponding Author

*E-mail: burdick2@seas.upenn.edu.

Author Contributions

†L.O. and C.B.H. contributed equally to this work.

Notes

The authors declare no competing financial interest.

■ ACKNOWLEDGMENTS

The authors acknowledge financial support from China Scholarship Council (File 201506210148), funding from a National Science Foundation MRSEC grant at the University of Pennsylvania, as well as a predoctoral fellowship (C.B.R.) and established investigator award (J.A.B.) from the American Heart Association.

■ REFERENCES

(1) Jungst, T.; Smolan, W.; Schacht, K.; Scheibel, T.; Groll, J. Strategies and Molecular Design Criteria for 3D Printable Hydrogels. *Chem. Rev.* **2016**, *116* (3), 1496−539.

(2) (a) Khalil, S.; Sun, W. Bioprinting endothelial cells with alginate for 3D tissue constructs. *J. Biomech. Eng.* **2009**, *131* (11), 111002. (b) Yan, Y.; Wang, X.; Pan, Y.; Liu, H.; Cheng, J.; Xiong, Z.; Lin, F.; Wu, R.; Zhang, R.; Lu, Q. Fabrication of viable tissue-engineered constructs with 3D cell-assembly technique. *Biomaterials* **2005**, *26* (29), 5864−71.

(3) (a) Ouyang, L.; Yao, R.; Mao, S.; Chen, X.; Na, J.; Sun, W. Three-dimensional bioprinting of embryonic stem cells directs high-throughput and highly uniformed embryoid body formation. *Biofabrication* **2015**, *7* (4), 044101. (b) Ouyang, L.; Yao, R.; chen, X.; Na, J.; Sun, W. 3D printing of HEK 293FT cell-laden hydrogel into macroporous constructs with high cell viability and normal biological functions. *Biofabrication* **2015**, *7* (1), 015010. (c) Boland, T.; Tao, X.; Damon, B. J.; Manley, B.; Kesari, P.; Jalota, S.; Bhaduri, S. Drop-on-demand printing of cells and materials for designer tissue constructs. *Mater. Sci. Eng., C* **2007**, *27* (3), 372−376.

(4) (a) Zhao, Y.; Yao, R.; Ouyang, L.; Ding, H.; Zhang, T.; Zhang, K.; Cheng, S.; Sun, W. Three-dimensional printing of Hela cells for cervical tumor model in vitro. *Biofabrication* **2014**, *6* (3), 035001. (b) Xu, T.; Gregory, C. A.; Molnar, P.; Cui, X.; Jalota, S.; Bhaduri, S. B.; Boland, T. Viability and electrophysiology of neural cell structures generated by the inkjet printing method. *Biomaterials* **2006**, *27* (19), 3580−8.

(5) (a) Lee, Y. B.; Polio, S.; Lee, W.; Dai, G.; Menon, L.; Carroll, R. S.; Yoo, S. S. Bio-printing of collagen and VEGF-releasing fibrin gel scaffolds for neural stem cell culture. *Exp. Neurol.* **2010**, *223* (2), 645−52. (b) Boland, T.; Mironov, V.; Gutowska, A.; Roth, E. A.; Markwald, R. R. Cell and organ printing 2: fusion of cell aggregates in three-dimensional gels. *Anat. Rec.* **2003**, *272* (2), 497−502.

(6) Yi, H. M.; Wu, L. Q.; Bentley, W. E.; Ghodssi, R.; Rubloff, G. W.; Culver, J. N.; Payne, G. F. Biofabrication with chitosan. *Biomacromolecules* **2005**, *6* (6), 2881−2894.

(7) Norotte, C.; Marga, F. S.; Niklason, L. E.; Forgacs, G. Scaffold-free vascular tissue engineering using bioprinting. *Biomaterials* **2009**, *30* (30), 5910−5917.

(8) Ozbolat, I. T.; Hospodiuk, M. Current advances and future perspectives in extrusion-based bioprinting. *Biomaterials* **2016**, *76*, 321−43.

(9) (a) Burdick, J. A.; Chung, C.; Jia, X.; Randolph, M. A.; Langer, R. Controlled degradation and mechanical behavior of photopolymerized hyaluronic acid networks. *Biomacromolecules* **2005**, *6* (1), 386−91. (b) Burdick, J. A.; Prestwich, G. D. Hyaluronic acid hydrogels for biomedical applications. *Adv. Mater.* **2011**, *23* (12), H41−56.

(10) Schuurman, W.; Levett, P. A.; Pot, M. W.; van Weeren, P. R.; Dhert, W. J. A.; Hutmacher, D. W.; Melchels, F. P. W.; Klein, T. J.; Malda, J. Gelatin-Methacrylamide Hydrogels as Potential Biomaterials for Fabrication of Tissue-Engineered Cartilage Constructs. *Macromol. Biosci.* **2013**, *13* (5), 551−561.

(11) Pescosolido, L.; Schuurman, W.; Malda, J.; Matricardi, P.; Alhaique, F.; Coviello, T.; van Weeren, P. R.; Dhert, W. J. A.; Hennink, W. E.; Vermonden, T. Hyaluronic Acid and Dextran-Based Semi-IPN Hydrogels as Biomaterials for Bioprinting. *Biomacromolecules* **2011**, *12* (5), 1831−1838.

(12) Skardal, A.; Devarasetty, M.; Kang, H. W.; Mead, I.; Bishop, C.; Shupe, T.; Lee, S. J.; Jackson, J.; Yoo, J.; Soker, S.; Atala, A. A hydrogel bioink toolkit for mimicking native tissue biochemical and mechanical properties in bioprinted tissue constructs. *Acta Biomater.* **2015**, *25*, 24−34.

(13) Highley, C. B.; Prestwich, G. D.; Burdick, J. A. Recent advances in hyaluronic acid hydrogels for biomedical applications. *Curr. Opin. Biotechnol.* **2016**, *40*, 35−40.

(14) (a) Kesti, M.; Muller, M.; Becher, J.; Schnabelrauch, M.; D'Este, M.; Eglin, D.; Zenobi-Wong, M. A versatile bioink for three-dimensional printing of cellular scaffolds based on thermally and photo-triggered tandem gelation. *Acta Biomater.* **2015**, *11*, 162−72. (b) Muller, M.; Becher, J.; Schnabelrauch, M.; Zenobi-Wong, M. Nanostructured Pluronic hydrogels as bioinks for 3D bioprinting. *Biofabrication* **2015**, *7* (3), 035006. (c) Skardal, A.; Zhang, J.; McCoard, L.; Xu, X.; Oottamasathien, S.; Prestwich, G. D. Photocrosslinkable hyaluronan-gelatin hydrogels for two-step bioprinting. *Tissue Eng., Part A* **2010**, *16* (8), 2675−85.

(15) Skardal, A.; Zhang, J. X.; Prestwich, G. D. Bioprinting vessel-like constructs using hyaluronan hydrogels crosslinked with tetrahedral polyethylene glycol tetracrylates. *Biomaterials* **2010**, *31* (24), 6173−6181.

(16) Skardal, A.; Zhang, J. X.; McCoard, L.; Oottamasathien, S.; Prestwich, G. D. Dynamically Crosslinked Gold Nanoparticle - Hyaluronan Hydrogels. *Adv. Mater.* **2010**, *22* (42), 4736.

(17) (a) Rodell, C. B.; Kaminski, A. L.; Burdick, J. A. Rational design of network properties in guest-host assembled and shear-thinning

DOI: 10.1021/acsbiomaterials.6b00158
ACS Biomater. Sci. Eng. XXXX, XXX, XXX−XXX

hyaluronic acid hydrogels. *Biomacromolecules* **2013**, *14* (11), 4125−34. (b) Rodell, C. B.; Wade, R. J.; Purcell, B. P.; Dusaj, N. N.; Burdick, J. A. Selective Proteolytic Degradation of Guest-Host Assembled, Injectable Hyaluronic Acid Hydrogels. *ACS Biomater. Sci. Eng.* **2015**, *1* (4), 277−286.

(18) Smeds, K. A.; Grinstaff, M. W. Photocrosslinkable polysaccharides for in situ hydrogel formation. *J. Biomed. Mater. Res.* **2001**, *54* (1), 115−21.

(19) Highley, C. B.; Rodell, C. B.; Burdick, J. A. Direct 3D Printing of Shear-Thinning Hydrogels into Self-Healing Hydrogels. *Adv. Mater.* **2015**, *27* (34), 5075−9.

(20) Rodell, C. B.; Mealy, J. E.; Burdick, J. A. Supramolecular Guest−Host Interactions for the Preparation of Biomedical Materials. *Bioconjugate Chem.* **2015**, *26*, 2279−89.

(21) Tous, E.; Ifkovits, J. L.; Koomalsingh, K. J.; Shuto, T.; Soeda, T.; Kondo, N.; Gorman, J. H., 3rd; Gorman, R. C.; Burdick, J. A. Influence of injectable hyaluronic acid hydrogel degradation behavior on infarction-induced ventricular remodeling. *Biomacromolecules* **2011**, *12* (11), 4127−35.

(22) Wade, R. J.; Bassin, E. J.; Rodell, C. B.; Burdick, J. A. Protease-degradable electrospun fibrous hydrogels. *Nat. Commun.* **2015**, *6*, 6639.

(23) Chung, C.; Beecham, M.; Mauck, R. L.; Burdick, J. A. The influence of degradation characteristics of hyaluronic acid hydrogels on in vitro neocartilage formation by mesenchymal stem cells. *Biomaterials* **2009**, *30* (26), 4287−96.

(24) Chopra, A.; Lin, V.; McCollough, A.; Atzet, S.; Prestwich, G. D.; Wechsler, A. S.; Murray, M. E.; Oake, S. A.; Kresh, J. Y.; Janmey, P. A. Reprogramming cardiomyocyte mechanosensing by crosstalk between integrins and hyaluronic acid receptors. *J. Biomech.* **2012**, *45* (5), 824−31.

DOI: 10.1021/acsbiomaterials.6b00158
ACS Biomater. Sci. Eng. XXXX, XXX, XXX−XXX